

05,13

## Bistability of magnetic skyrmions in a multilayer ferromagnetic/heavy metal structure

© V.A. Gubanov<sup>1</sup>, M. Mruczkiewicz<sup>2</sup>, A.V. Sadovnikov<sup>1</sup>

<sup>1</sup> Saratov National Research State University,  
Saratov, Russia

<sup>2</sup> Institute of Electrical Engineering SAS, Dúbravská cesta 9, 841 04,  
Bratislava, Slovak Republic

E-mail: vladmeen@gmail.com

Received April 29, 2022

Revised April 29, 2022

Accepted May 12, 2022

The effect of the Dzyaloshinskii-Moriya interface interaction on the stability of magnetic skyrmions in the ferromagnet-heavy metal multilayer structure depending on the number of multilayer repetitions was investigated by micromagnetic modeling. The parameters of the multilayer structure for the stabilization of magnetic skyrmions in nanodisks formed by Ir/Co/Pt layers are selected. It is shown how the value of the Dzyaloshinskii-Moriya exchange interaction affects the type, stability, and radius of magnetic skyrmions in multilayer nanopillars. The results obtained can be used to create devices for processing and storage information signals.

**Keywords:** spin waves, magnonics, magnetic skyrmions, ferromagnetic, heavy metal, Dzyaloshinskii-Moriya interaction, multistability.

DOI: 10.21883/PSS.2022.09.54165.19HH

### 1. Introduction

The study of stabilization of magnetic vortices is of great interest in view of the consideration of methods of formation of nanodimensional cylinders, including those with a curvilinear cross-section profile [1]. In the field of magnetic materials, magnetic vortices called skyrmions are being actively investigated. Due to its small size and topological stability when interacting with other stable magnetization states, a skyrmion can be used in high-density memory devices [2].

Skyrmions can be stabilized in nanometer films due to an external magnetic field, perpendicular anisotropy and interfacial Dzyaloshinskii-Moriya interaction, hereinafter called DMI which occurs at the ferromagnetic/heavy metal boundary [3,4]. In the case of multilayer structures, there is an additional contribution from the dipole interaction [5,6]. It has been found that by reducing the geometric dimensions of the layers it is possible to increase the skyrmion stability [7]. It has also been experimentally shown that the created magnetic skyrmions can be stable at room temperature [8,9]. The formation of skyrmion structures is possible by means of a magnetic-force microscopy tip, in which a magnetic perturbation in the structure is caused [10,11]. For example, this was presented for the Pt/Co/Pt structure [12–14].

The results of micromagnetic modelling of multilayer structures with repeated ferromagnetic/heavy metal layers are presented in this paper. The effect of multistability of magnetic skyrmions at a change of value of exchange interaction is shown. Separately, the magnitude

of Dzyaloshinskii-Moriya interaction influences the transformation of the type of skyrmion in the studied structure.

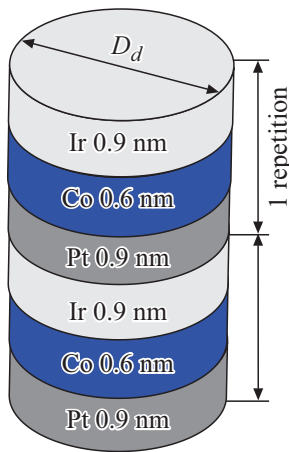
### 2. The studied structures and numerical modelling

Fig. 1 shows a schematic representation of a multilayer ferromagnetic/heavy metal structure. Three layers alternate in the structure: Ir/Co/Pt. Later on, the material parameters were averaged and the three layers were replaced with one multilayer of ferromagnetic, i.e., a skyrmion occurs in the ferromagnetic layer.

The diameter of the  $D_{\text{extd}}$  was 200 nm, the thickness of the structure depended on the number of repetitions  $n$ . For the real structure, the thickness of the multilayer was 2.4 nm (Ir = 0.9 nm, Co = 0.6 nm, Pt = 0.9 nm), while the micromagnetic simulation program was 0.6 nm (only the ferromagnet thickness was used).

Micromagnetic simulation was carried out in the MuMax3 [15] software package, which solves the Landau-Lifshitz-Gilbert equation [16]: The number of repetitions ranged from 2 to 4. The value of the DMI interaction varied in the range of 0–1.2 mJ/m<sup>2</sup>, which is consistent with the experimental data [6,17–21].

The resulting skyrmions have a characteristic such as the skyrmion diameter  $D_{\text{sk}}$ . This value depends on both the DMI and the number of multilayers.  $D_{\text{sk}}$  was measured as follows: a diameter cut was taken and the back position was approximately 0 (lying in the film plane). Such positions in the cut will be two in the case of a stabilized skyrmion.



**Figure 1.** The image of the studied structure.

It should also be noted that emerging skyrmions can be of different types — Neel and Bloch [22].

In micromagnetic simulation, it was found that in magnetic nanostructures, the same type of skyrmion can be produced, but with different spin direction — so called clockwise and counterclockwise direction (in future will be denoted as R and L for the Neel type of skyrmion, B and C — for the Bloch skyrmion).

Fig. 2 shows the relationship of the skyrmion diameter to the diameter of a nanodot  $D_{sk}/D_d$  to the DMI value for a 6 repetition structure. The following steps were taken to obtain this dependence. The initial value of DMI was assumed to be  $0.03 \text{ mJ/m}^2$  (a small deviation in this interaction is needed) a, skyrmion originated, system relaxation occurred, and the diameter of the skyrmion was measured. The resulting magnetization distribution was used as a baseline state to further increase the DMI value in small increments ( $0.003 \text{ mJ/m}^2$ ) to  $1.2 \text{ mJ/m}^2$ . Also at each step the definition of the skyrmion type (R, L, B or C) was made. As you can see in Fig. 2, in this structure, there is a 4 multilayer transformation of the skyrmion type from R into type L via an intermediate skyrmion of type C and for each existing skyrmion, three areas (I — I, C — II, R — III) are allocated. This may indicate that with a specific DMI value, we can observe this skyrmion configuration, which can then be used as a combination to encode data.

However, in addition to the phenomenon of changing the type of skyrmion when changing the DMI value, the multistable character of the multilayer structure was also shown. To demonstrate this effect, a micromagnetic simulation was conducted for the structure with a repetition of multilayers of  $n = 2$  and  $n = 4$ . To identify the multistability state, in addition to the step-by-step increase of DMI values (on Figs. 3 and 4 shown in red), at  $1.2 \text{ mJ/m}^2$  there was a step-by-step reduction of DMI values (on Figs. 3 and 4 shown in blue). For the case of  $n = 2$ , there is a multistability area in the range of  $0.34\text{--}0.55 \text{ mJ/m}^2$ . As you can see

on the inset for Fig 3, *a*, as DMI increases, the skyrmion in the second layer from R-type transforms into L-type with an intermediate value C, and when the DMI value decreases — from L-type to R-type via B. In this case, when the value changes directly and inversely, different relationships of  $D_{sk}/D_d$  are observed in the multistability area of DMI.

With the number of repetitions of  $n = 4$  multilayers, there was a shift of the multistability region into a higher range of values of DMI interaction (from  $0.8 \text{ mJ/m}^2$  to  $1.2 \text{ mJ/m}^2$ ), and with a value of DMI  $0.4 \text{ mJ/m}^2$ , the curve inclination change occurs. If you consider changing the type of skyrmion in the multilayer, then at the value of DMI  $0.4 \text{ mJ/m}^2$  the type of skyrmion changes from R to L when increasing DMI and L to R at a decrease of DMI of 3 multilayer. This process takes place without a multistable state.

Since these skyrmions are stable magnetization configurations, a micromagnetic simulation has been performed, in which dependences of the total energy  $E_{total}$  on the DMI value were obtained. Figs. 3, *b* and 4, *b* shows the total energy dependences of the system for the quantity of repetitions of layers  $n = 2$  and  $n = 4$ .

These graphs present  $E_{total}$  values with negative values. This can be regarded as ( $E_{total} = 0 \text{ J}$ ) equilibrium deviation. A change in energy indicates the formation of skyrmion structures. When comparing the received graphs, you should pay attention to the values  $E_{total}$  in case of  $n = 2$  and  $n = 4$ . For  $n = 2$   $E_{total}$  changes in the range of  $(-0.4) \div (-1.6) \cdot 10^{-18} \text{ J}$ , and for  $n = 4$  — in the range of  $(-2.75) \div (-4.5) \cdot 10^{-18} \text{ J}$ . When comparing these values, it is possible to understand that as the layers increase, the energy of the system increases.

Also, values of DMI, in which there is a transformation of the type of skyrmion and showing the relationship between

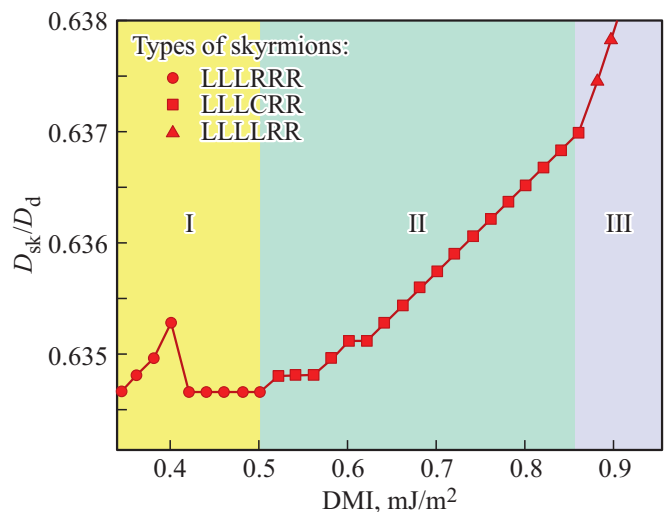


**Figure 2.** Plot of the relationship between  $D_{sk}/D_d$  and the DMI interaction value. Areas with different types of skyrmions in the third layer: I — LLRR, II — LLCR, III — LLLR.

the change of  $D_{\text{texts}k}$  and  $E_{\text{exttotal}}$  are marked with a gray dotted line on Figs. 3 and 4. Thus, for  $n = 2$  there is 1 DMI value, while for  $n = 4$  — 2 DMI values.

As described earlier, in some cases, a change in the type of skyrmion can occur with a bistability effect, in which there is also a bistable change in the energy of the system.

You can see that, as with  $D_{\text{sk}}/D_d$  dependences on DMI, there are 3 areas: 1 area from 0 to 0.4 mJ/m<sup>2</sup> for both straight and return pass the total energy of the system remains the same and at the critical value of 0.5 mJ/m<sup>2</sup>, as seen in Fig. 4, *a*, there is a transformation of the type of skyrmion in 3 layer. With this transformation, the total energy of the system changes as the inclination of the curve changes (in the range from 0.5 to 1.2 mJ/m<sup>2</sup>). Starting from 0.8 mJ/m<sup>2</sup>, there is a multistability area where you can see a bidirectional change in the skyrmion radius as well as the total energy of the system.

Thus, multistability can be observed by changing the total energy of the system. In this case, multistable modes of formation of skyrmions of different types in layers of

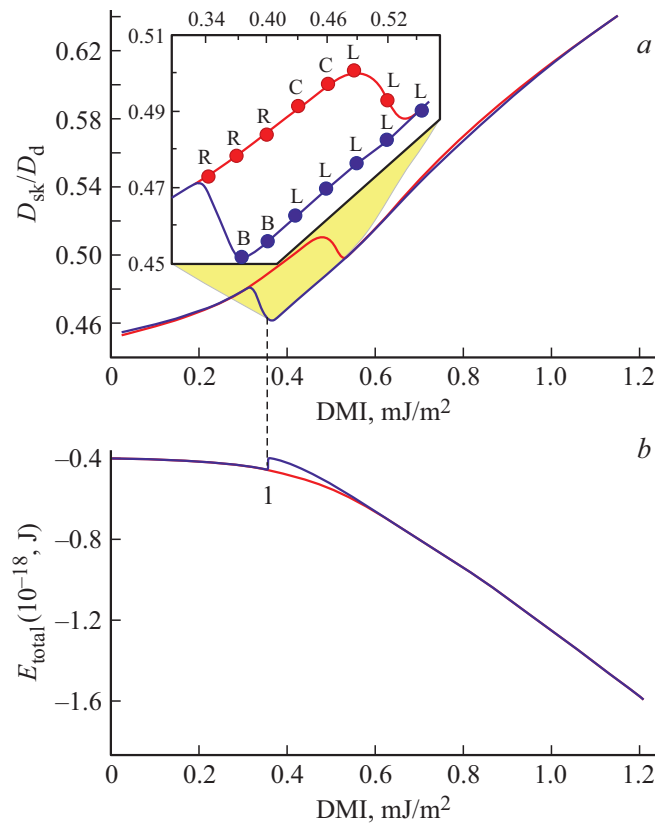


**Figure 3.** *a*) Plot of the dependence of ratio  $D_{\text{sk}}/D_d$  and the DMI interaction value in the structure with the quantity of layers  $n = 2$ . The red color (the top part) shows the dependence plotted when increasing the value of DMI interaction, while the blue color (the lower part) — when decreasing the DMI value. On the inset: multistability mode — change of the skyrmion type in the second multilayer when increasing and decreasing DMI. *b*) The dependence of the total energy  $E_{\text{total}}$  of the system on the DMI value. The digit 1 indicates the moment of switching.

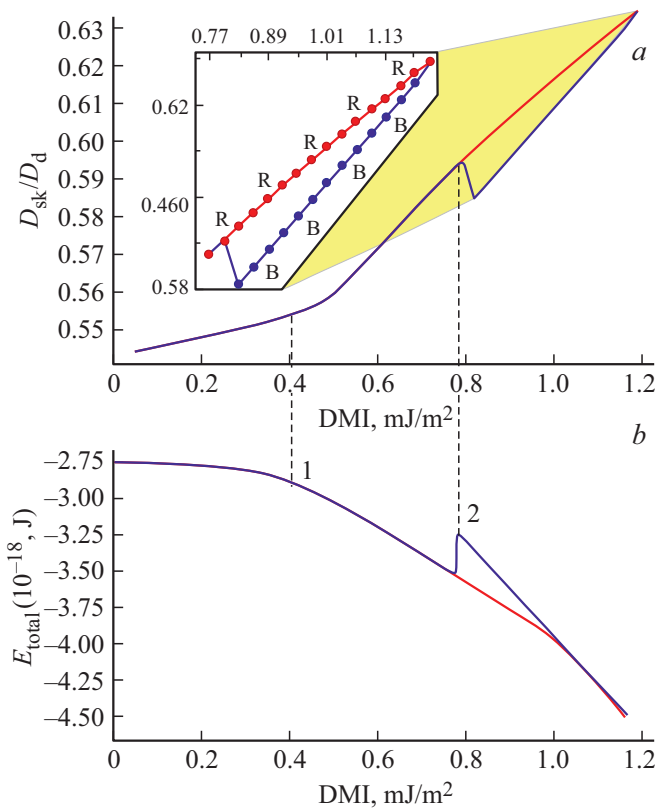


**Figure 4.** *a*) Plot of the dependence of ratio  $D_{\text{sk}}/D_d$  and the DMI interaction value in the structure with the quantity of layers  $n = 4$ . The red color (the top part) shows the dependence plotted when increasing the value of DMI interaction, while the blue color (the lower part) — when decreasing the DMI value. On the inset: multistability mode — change of the skyrmion type in the second multilayer when increasing and decreasing DMI. *b*) The dependence of the total energy  $E_{\text{total}}$  of the system on the DMI value. The numbers 1 and 2 indicate the moment of switching (1 — switching without the bistability effect, 2 — with bistability).

multilayer structure can be observed with values of the constant of interface interaction of Dzialoshinskii–Moriya, which could lead to the early identification of the detected effect in an experimental study. In this case, the use of multilayer nanodisks allows to observe the processes of formation and stabilization of skyrmions [23] by atomic-force microscopy methods.

### 3. Conclusion

Thus, by means of numerical modeling the influence of the value of Dzialoshinskii–Moriya interaction on the stability of magnetic skyrmions in the multilayer structure of the ferromagnetic/heavy metal is studied, depending on the amount of repetition of multilayers. The parameters of multilayer structure have been selected to stabilize magnetic skyrmions in the multilayer structure Ir/Co/Pt. It is shown how, when DMI value changes with the subsequent skyrmion type transformation,  $D_{\text{sk}}/D_d$  and  $E_{\text{total}}$  change.

The multistability modes in the multilayer structure Ir/Co/Pt are shown. The obtained results can be used for creating information signal processing and storage devices.

### Funding

The study was performed with the support of the Ministry of Education and Science of Russia as part of the Government Task (project No. FSR-2020-0005).

### Conflict of interest

The authors declare that they have no conflict of interest.

### References

- [1] K. Bublikov, J. Tóbi, A.V. Sadovnikov, M. Mruczkiewicz. *J. Magn. Magn. Mater.* **537**, 168105 (2021).
- [2] K. Everschor-Sitte, J. Masell, R.M. Reeve, M. Kläui. *J. Appl. Phys.* **124**, 240901 (2018).
- [3] N. Romming, C. Hanneken, M. Menzel, J.E. Bickel, B. Wolter, K. von Bergmann, A. Kubetzka, R. Wiesendanger. *Science* **341**, 636 (2013).
- [4] H. Yang, A. Thiaville, S. Rohart, A. Fert, M. Chshiev. *Phys. Rev. Lett.* **115**, 26, 267210 (2015).
- [5] F. Büttner, I. Lemesch, G.S.D. Beach. *Sci. Rep.* **8**, 1 (2018).
- [6] M. Zelent, J. Tóbi, M. Krawczyk, K.Y. Guslienko, M. Mruczkiewicz. *Phys. Status Solidi (RRL) Rapid Res. Lett.* **11**, 1700259 (2017).
- [7] S. Rohart, A. Thiaville. *Phys. Rev. B* **88**, 184422 (2013).
- [8] K. Zeissler, M. Mruczkiewicz, S. Finizio, J. Raabe, P. Shepley, A.V. Sadovnikov, S.A. Nikitov, K. Fallon, S. McFadzean, S. Mcvitie, T.A. Moore, G. Burnell, C.H. Marrows. *Sci. Rep.* **7**, 15125 (2017).
- [9] V. Karakas, A. Gokce, A.T. Habiboglu, S. Arpacı, K. Ozbozduman, I. Cinar, C. Yanik, R. Tomasello, S. Tacchi, G. Siracusano. *Sci. Rep.* **8**, 7180 (2018).
- [10] A. Casiraghi, H. Corte-León, M. Vafaei, F. Garcia-Sanchez, G. Durin, M. Pasquale, G. Jakob, M. Kläui, O. Kazakova. *Commun. Phys.* **2**, 1 (2019).
- [11] A.I. Bezverkhniy, V.A. Gubanov, A.V. Sadovnikov, R.B. Morgunov. *FTT* **63**, 12.2053 (2021) (in Russian).
- [12] V.L. Mironov, R.V. Gorev, O.L. Ermolaeva, N.S. Gusev, Y. Petrov. *Phys. Solid State* **61**, 1594 (2019).
- [13] M.V. Sapozhnikov, R.V. Gorev, E.V. Skorokhodov, N.S. Gusev, A.V. Sadovnikov, O.G. Udalov. *Phys. Rev. B* **105**, 024405 (2022).
- [14] N.S. Gusev, A.V. Sadovnikov, S.A. Nikitov, M.V. Sapozhnikov, O.G. Udalov. *Phys. Rev. Lett.* **124**, 157202 (2020).
- [15] A. Vansteenkiste, J. Leliaert, M. Dvornik, M. Helsen, F. Garcia-Sanchez, B.V. Waeyenberge. *AIP Advances* **4**, 107133 (2014).
- [16] L. Landau, E. Lifshitz. *Phys. Z. Sow.* **8**, 153 (1935).
- [17] K. Gerlinger, B. Pfau, F. Büttner, M. Schneider, L.-M. Kern, J. Fuchs, D. Engel, C.M. Günther, M. Huang, I. Lemesch, L. Caretta, A. Churikova, P. Hessler, C. Klose, C. Strüder, C. von Korff Schmising, S. Huang, A. Wittmann, K. Litzius, D. Metternich, R. Battistelli, K. Bagschik, A. Sadovnikov, G.S.D. Beach, S. Eisebitt. *Appl. Phys. Lett.* **118**, 192403 (2021).
- [18] A.V. Ognev, A.G. Kolesnikov, Yong Jin Kim, In Ho Cha, A.V. Sadovnikov, S.A. Nikitov, I.V. Soldatov, A. Talapatra, J. Mohanty, M. Mruczkiewicz, Y. Ge, N. Kerber, F. Dittrich, P. Virnau, M. Kläui, Young Keun Kim, A.S. Samardak. *ACS Nano* **14**, 11, 14960 (2020).
- [19] A.S. Samardak, A.V. Davydenko, A.G. Kolesnikov, A.Yu. Samardak, A.G. Kozlov, Bappaditya Pal, A.V. Ognev, A.V. Sadovnikov, S.A. Nikitov, A.V. Gerasimenko, In Ho Cha, Yong Jin Kim, Gyu Won Kim, O.A. Tretiakov, Young Keun Kim. *NPG Asia Mater.* **12**, 51 (2020).
- [20] S. Finizio, S. Wintz, K. Zeissler, A.V. Sadovnikov, S. Mayr, S.A. Nikitov, C.H. Marrows, J. Raabe. *Nano Lett.* **19**, 1, 375 (2019).
- [21] I.L. Kalentyeva, O.V. Vikhrova, Yu.A. Danilov, M.V. Dorokhin, Yu.A. Dudin, A.V. Zdoroveishchev, A.V. Kudrin, M.P. Temiryazeva, A.G. Temiryazev, S.A. Nikitov. *FTT* **61**, 9, 1694 (2019) (in Russian).
- [22] W. Kang, Y. Huang, X. Zhang, Y. Zhou, W. Zhao. *Proc. IEEE* **104**, 10, 2040 (2016).
- [23] Iu.V. Vetrova, M. Zelent, J. Šoltýs, V.A. Gubanov, A.V. Sadovnikov, T. Šcepka, J. Dérier, R. Stoklas, V. Cambel, M. Mruczkiewicz. *Appl. Phys. Lett.* **118**, 212409 (2021).